Available online at www.sciencedirect.com

ScienceDirect

Ceramics International 40 (2014) 1919–1925

CERAMICS INTERNATIONAL

www.elsevier.com/locate/ceramint

Crystal structure and highly enhanced ferroelectric properties of (Tb, Cr) co-doped $BiFeO_3$ thin films fabricated by a sol–gel method

Guohua Dong, Guoqiang Tan*, Wenlong Liu, Ao Xia, Huijun Ren

Key Laboratory of Auxiliary Chemistry & Technology for Chemical Industry, Ministry of Education, Shaanxi University of Science & Technology, Xi'an, Shaanxi 710021, China

Received 24 June 2013; received in revised form 18 July 2013; accepted 18 July 2013
Available online 26 July 2013

Abstract

$BiFeO_3$ (BFO), Tb-doped $BiFeO_3$ (BTFO) and Tb–Cr co-doped $BiFeO_3$ (BTFCO) thin films were successfully prepared on SnO_2: F (FTO)/glass substrates by a sol–gel method. The influence of Tb and Cr co-doping on the structure, leakage current, charge defects, dielectric and ferroelectric properties of the BTFCO thin film was investigated systematically. X-ray diffraction (XRD) and Raman spectroscopy results clearly reveal the structure transition and (110) preferentially oriented film texture for the co-doped thin film. BTFCO thin film becomes more compact structure and uniform than that of the other two films. The improved electrical properties of BTFCO thin film are observed in comparison with the BFO thin film. Furthermore, the highly enhanced ferroelectric property with a giant remanent polarization ($2P_r = 161.60\ \mu C/cm^2$) and the decreased leakage current density (3.76×10^{-5} A/cm^2 at 200 kV/cm) via co-doping Tb and Cr are obtained. The X-ray photoelectron spectroscopy (XPS) analyses clarify that the ratios of Fe^{2+}/Fe^{3+} in the BFO and BTFCO thin films are calculated as 45:55 and 26:74, respectively, which indicate that the presence of Fe^{2+} ions is suppressed with co-doping Tb and Cr.

Keywords: C. Ferroelectric properties; Multiferroic; $BiFeO_3$ thin film; Co-doped

1. Introduction

Multiferroic materials with ferroelectricity and antiferromagnetism in the same phase have attracted great attention due to their potential applications in multifunctional devices [1]. One of the interesting multifunctional materials is $BiFeO_3$ and it is the only known material exhibiting good ferroelectromagnetism at room temperature, because of a high Curie temperature (1043 K) and a high Neel temperature (647 K) [2,3]. Besides pulsed-laser deposition (PLD) and RF sputtering [3,4], a large remanent polarization (P_r) in BFO thin films prepared by a sol–gel method has also been reported in previous literatures [5,6] which has many advantages in mass production of thin films, such as easy control of stoichiometry, low processing temperature, and low cost. However, the limitation for the applications of $BiFeO_3$ films is large leakage current density at room temperature. So, the highly conductive nature of $BiFeO_3$ makes it difficult to obtain the excellent ferroelectric properties [7]. In particular, it has been strongly suggested that the site-engineering concept should be applied to the decrease leakage current density and to improve the ferroelectric properties of BFO thin films [8].

A- and B-sites of co-doped BFO thin films have been widely investigated recently, in which Bi^{3+} in the A-site was partially replaced by La^{3+} or Nd^{3+} [9] while Fe^{3+} in the B-site was partially replaced by high-valence Mn^{4+}, V^{5+}, or Mo^{6+} simultaneously [10–13]. Hong et al. have reported that the leakage current density of BFO films could be decreased by Sm–Ti co-substitution (1.5×10^{-5} A/cm^2 at 300 kV/cm) [14]. Wen et al. reported that the improved ferroelectric property was found in BFO thin films co-substituted with Pr/Mn and the film showed a large remanent polarization of 62 μC/cm^2 and a reduced coercive field of 217 kV/cm [15]. However, some studies also denoted that substitution of ions with higher (lower) valence for Fe^{3+} ions in BFO thin films would produce cation vacancies or anion vacancies [16].

Upon the above, Tb^{3+} and Cr^{3+} were chosen as the appropriate candidates to substitute Bi^{3+} and Fe^{3+} in BFO thin films, respectively. Thus, it was expected that Tb and Cr

*Corresponding author. Tel.: +8613759878391.
E-mail address: tan3114@163.com (G. Tan).

0272-8842/$ - see front matter © 2013 Elsevier Ltd and Techna Group S.r.l. All rights reserved.
http://dx.doi.org/10.1016/j.ceramint.2013.07.099

co-doping would further enhance the ferroelectric properties of BFO thin films. In this paper, Tb and Cr co-doped $BiFeO_3$ thin films were synthesized: part of Bi^{3+} ions was substituted by Tb^{3+}, and part of Fe^{3+} was substituted by Cr^{3+}. The films were grown on FTO/glass substrates by a sol–gel method. Electrical properties of Tb and Cr co-substituted BFO thin films have been measured. In addition, the effects of co-substitution on the electrical properties, such as the improved dielectric property and ferroelectric property have been demonstrated.

2. Experimental

The pure $BiFeO_3$ (BFO), $Bi_{0.89}Tb_{0.11}FeO_3$ (BTFO) and $Bi_{0.89}Tb_{0.11}Fe_{0.98}Cr_{0.02}O_3$ (BTFCO) thin films were prepared by a sol–gel method. For the preparation of $Bi_{1-x}Tb_xFe_{1-y}Cr_yO_3$ precursor solutions, $Tb(NO_3)_3 \cdot 6H_2O$, $Cr(NO_3)_3 \cdot 9H_2O$, $Fe(NO_3)_3 \cdot 9H_2O$ and $Bi(NO_3)_3 \cdot 5H_2O$ were used as the starting materials. To compensate for Bi loss during the annealing process, 5 mol% excess $Bi(NO_3)_3 \cdot 5H_2O$ was added. These solutions were mixed in 2-methoxyethanol. Acetic anhydride was used as the dehydrating agent. The volume ratio of 2-methoxyethanol and acetic anhydride was 3:1. Ethanol amine was used to adjust the viscosity. The concentration of cations was adjusted to 0.3 mol/L by the addition of 2-methoxyethanol. The solutions were stirred at room temperature for 2 h to obtain the homogeneous precursor solutions. The above processes were performed in an ambient atmosphere. FTO/glass was used as the substrate. Depositions were carried out by spin-coating with a speed of 4000 rpm. The deposited wet films were preheated at 200 °C on a hot plate for 5 min. The dried films were inserted into a furnace at 550 °C under an air atmosphere for crystallization. These procedures were repeated 14 times to obtain the desired thickness of films. In order to measure the electrical properties, Au top electrodes (with areas of 0.502 mm^2) were deposited on the top surface of the thin films by ions sputtering through a metal shadow mask. After annealing at 300 °C for 20 min, the electrodes could completely contact with the film. Hence, a capacitor was obtained, and it was ready for electric properties tests.

The prepared films were studied by a range of characterization methods. Japan Rigaku Company D/max-2200 X-ray diffractometer was used to identify the structure and crystallinity of the thin films. With Cu target, the scanning step length was 0.02° and operated at 40 kV and 40 mA. The initial angle was 15° and the end angle was 70°. Raman spectroscopy measurements were performed by a Horiba JYHR800 Raman system equipped with an Ar ion laser excitation at 514.5 nm. Laser power was kept below 20 mW to avoid local heating effects. The micromorphology and thickness of the films were observed by a field emission scanning electron microscopy (FE-SEM, JSM-6700, JEOL, Japan). The electric hysteresis loops and the leakage current were tested by an aix ACCT TF-Analyzer 2000. DC voltage range was 0–15 V, voltage step was 0.5 V and the delay time was 1 s. Agilent E4980A Precision LCR Meter was used to measure the dielectric properties of the thin films. The oxidation states of Fe ions were investigated on surface of BFO and BTFCO thin films by X-ray photoelectron spectroscopy (XPS, XSAM800, Kratos Ltd., Britain) and all binding energies were calibrated with respect to C1s spectral line at 284.6 eV.

3. Results and discussion

Fig. 1a shows XRD patterns of BFO, BTFO and BTFCO thin films prepared on FTO/glass substrates. Fig. 1b shows the magnifications in the vicinities of 2θ values of 32.0° and 57°, respectively. All the films exhibit a polycrystalline perovskite structure without secondary phases. The magnified XRD patterns of BTFO film exhibit the merging of the (104) and (110) peaks compared to the BFO counterpart, indicating that a structural transition is created by 11% Tb-doping. However, with the Tb and Cr co-doping, there are the remarkable changes in the diffraction patterns. The (104) peak disappears completely, while a high preferred orientation appears along (110) crystal plane for the BTFCO thin film. From the

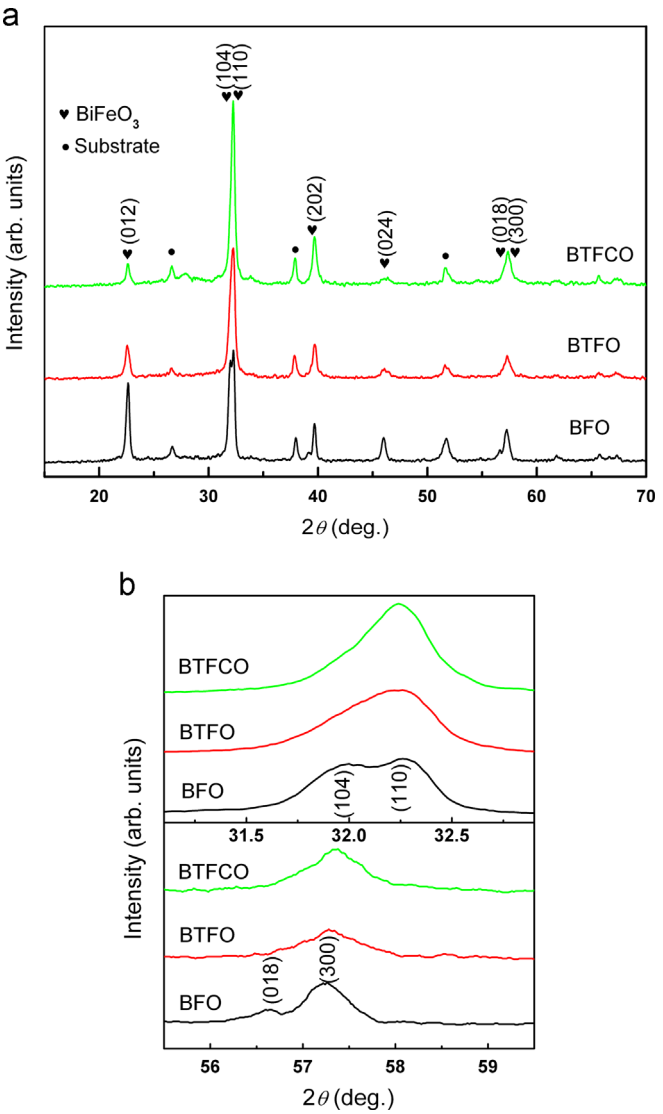

Fig. 1. a XRD patterns of BFO, BTFO and BTFCO thin films. b XRD patterns in the range of 2θ from 31° to 33° and 55° to 60°.

magnified XRD patterns, the (018) peak just vanishes and the (300) peak becomes broad with doping Tb and Cr. XRD peaks changing upon Tb-doping were previously reported as the signature of structure transition [17]. Furthermore, the structural transition is resulted from the relatively small ionic radius of the Tb^{3+} (0.923 Å) and Cr^{3+} (0.615 Å) ions compared to that of Bi^{3+} (1.03 Å) and Fe^{3+} (0.645 Å), respectively.

On the one hand, the co-doping of the rare earth and transition metal ions can lead to the structural transition of BFO thin films and the results are changed in the macroscopic polarization [17]. On the other hand, the co-doping BTFCO thin film shows the (110) preferred orientation as deposited on FTO/glass substrate [18]. Therefore, the large polarization is reasonably desired in the current work.

The limited X-ray diffraction patterns do not provide clear and enough information about the effect of co-doping on the BFO structure. The structure transition caused by the rare earth (Tb^{3+}) and transition metal (Cr^{3+}) ions co-doping in the BFO is further studied by Raman spectroscopy. Fig. 2 shows the Raman spectroscopy of the BFO, BTFO and BTFCO thin films measured at room temperature. All of the Raman modes observed in the BFO thin film are identical to the rhombohedrally distorted perovskite structure [19]. The peak position is determined by the Lorentzian fitting as listed in Table 1. Almost the Raman peaks of BTFO and BTFCO are shifted to higher frequencies in comparison with BFO. The *E*-1 mode associates with Fe ions and A_1-1 mode is related to Bi ions [20]. The larger shift of the A_1-1 mode of BTFO to higher frequency shows that Tb ions doping can produce significant structural transition on Bi-sites. The peak positions of BTFCO shift to low frequencies, and it can be attributed to the incorporation of Cr^{3+} ions at Fe-sites. Higher frequency Raman modes are generally related to the vibrational modes involving oxygen [20]. For the BTFCO, the Raman spectra show quite different features from BFO. As shown in Table 1,

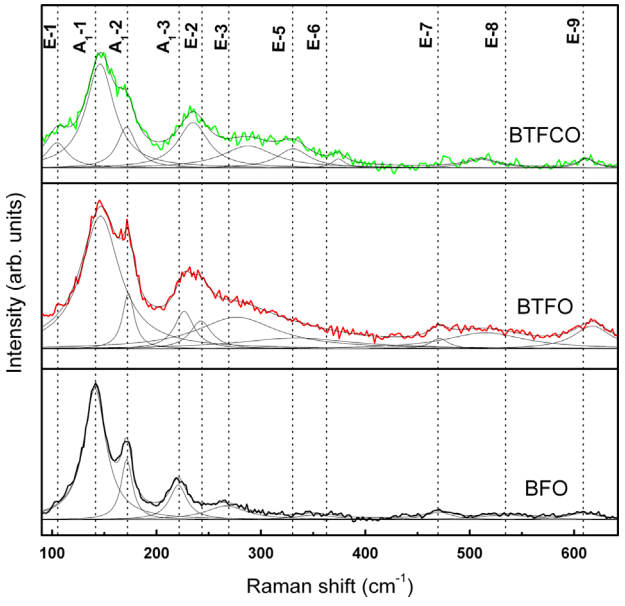

Fig. 2. Raman spectra of BFO, BTFO and BTFCO thin films.

Table 1
A_1 and *E* modes for the BFO, BTFO and BTFCO thin films.

Samples	Assigned Raman modes (cm^{-1})									
	E-1	A_1-1	A_1-2	A_1-3	*E*-2	*E*-3	*E*-5	*E*-6	*E*-7	*E*-8	*E*-9
BFO	–	142	172	221	–	266	–	352	471	535	608
BTFO	–	147	174	226	243	277	334	–	471	514	618
BTFCO	104	145	172	236	–	288	332	375	–	511	612

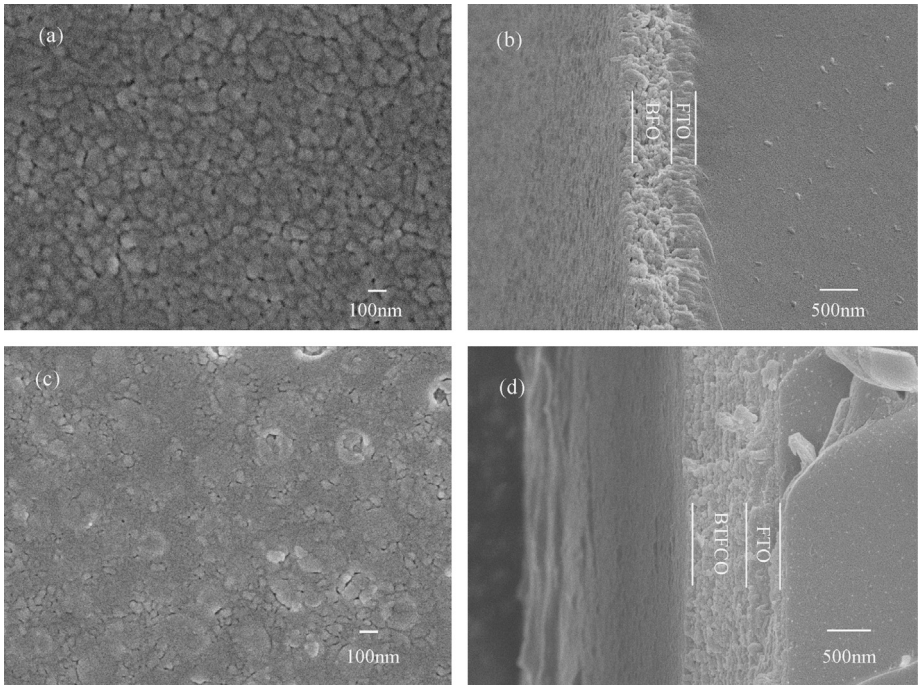

Fig. 3. Surface and cross-sectional images of the BFO (a, b) and BTFCO (c, d) thin films.

the *E*-3 and *A*-3 modes of BTFCO shift to the higher frequency compared to that of the BFO, while the *E*-5 mode emerges from the Raman spectroscopy. All these results indicate the more rotation of the oxygen octahedra is caused by the structure transition [20].

Fig. 3 shows the surface morphologies and the cross-sectional micrographs of BFO and BTFCO thin films, respectively. The morphological differences have been clearly observed in the co-doped thin films compared to the pure BFO. Large grains and some wide pores between the grains are observed in the pure BFO. However, BTFCO thin film exhibits that the Tb–Cr co-doping has a significant effect on the surface morphology and grain size. BTFCO thin film shows a relatively dense structure and improves uniformity of the grain size in comparison with the BFO thin film. In the co-doped thin films, the grain size is found to be reduced and the smaller grains are aggregated as grains-cluster. The decrease of grain size in the co-doped thin films can be interpreted by the suppression of oxygen vacancy concentration, which results in slower oxygen ion motion and consequently lowers the grain growth rate [21,22]. At the same time, the surface blows up many little bubbles. The little bubbles may be derived from the unit cell distortion by co-doping Tb and Cr.

The typical dielectric properties of the BFO, BTFO and BTFCO thin films are measured at room temperature by varying the frequencies from 1 kHz to 1 MHz. As shown in Fig. 4a, the dielectric constants of the thin films are gradually decreased with the increase of frequency. The dielectric constants of the BFO, BTFO and BTFCO thin films are 116, 158 and 160 at the applied frequency of 1 MHz, respectively. The dielectric losses (Fig. 4b) of the pure BFO, BTFO and BTFCO thin films are 0.17, 0.13 and 0.14 at 1 MHz, respectively. The high dielectric constant and low dielectric loss of BTFO and BTFCO thin films are correlated with the large remnant polarization and the low leakage current density. As the frequency increases, the dielectric constants of BTFO thin film decreased dramatically, which is believed to be related to the increased contribution of DC conductivity due to the space charges near the interfaces. The decrease of the dielectric constants at the high frequency is attributed to the fact that the polarizations with large relaxation times cease to respond [23]. Moreover, in the high frequency section all the thin films have the dramatic increase of the dielectric loss. These results may be from two aspects: dipole resonance and the differences between the top and bottom electrodes.

Fig. 5 shows leakage current density versus electric field characteristics of BFO, BTFO and BTFCO thin films at positive bias measured at RT. From the leakage current density analysis, the leakage current density value of BTFCO thin film is two orders lower than that of BFO thin film. The measured leakage current density of the BFO thin film is 1.43×10^{-3} A/cm^2 at the applied electric field of 200 kV/cm. The large leakage current mainly results from the oxygen vacancies and iron valence (Fe^{2+}, Fe^{3+}), as well as from various defects such as stoichiometry, pores, cracks and interstices in the films [24]. At the same applied electric field, the leakage current density of BTFCO thin film is 3.76×10^{-5} A/cm^2. It is well documented that the presence of a small amount of rare earth ions at Bi sites suppresses volatilization of Bi ions and stabilizes the perovskite structure [25]. One reason could be due to control of the valence fluctuation and the reduction of oxygen vacancies, which will be further explained in the

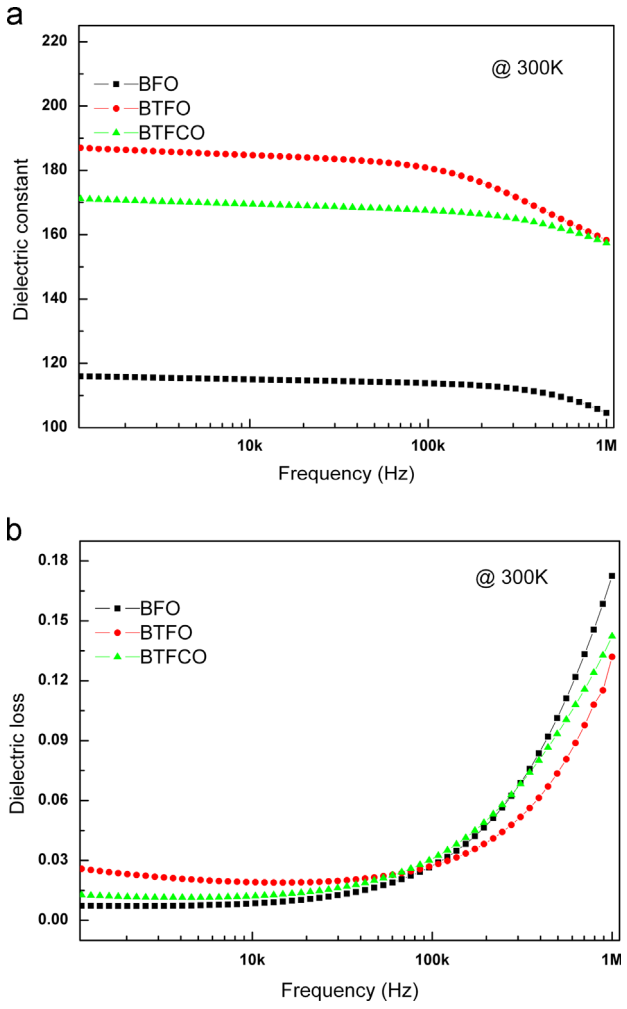

Fig. 4. Relationship between frequencies and a dielectric constants and b dielectric losses of BFO, BTFO and BTFCO thin films.

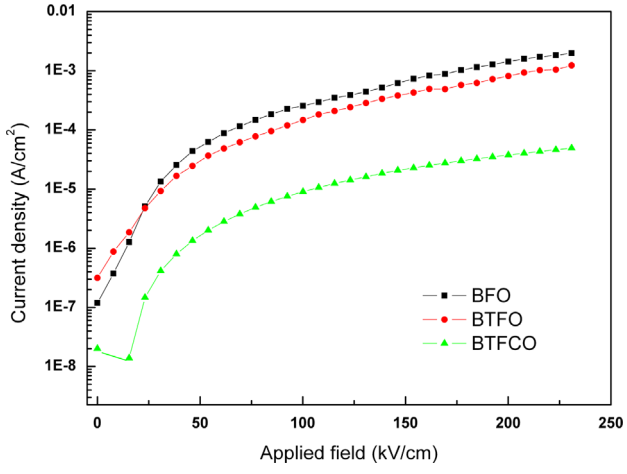

Fig. 5. Leakage current densities of BFO, BTFO and BTFCO thin films.

following XPS results analysis. In addition, the co-doping also makes the contribution to the denseness of microstructure and reduces the leakage current density.

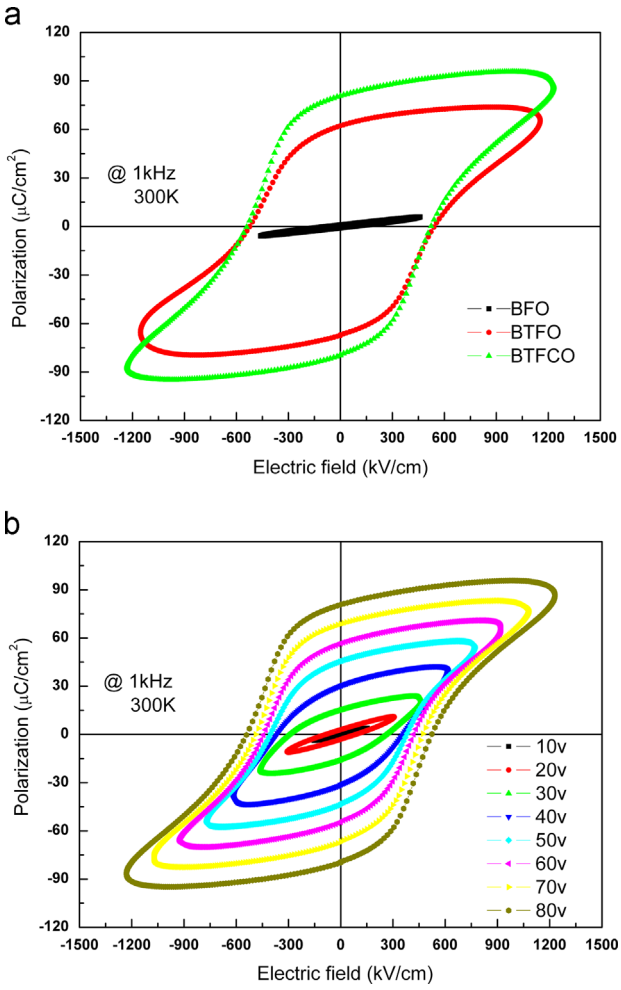

Fig. 6. a Ferroelectric *P–E* hysteresis loops of the BFO, BTFO and BTFCO thin films and b evolution of *P–E* hysteresis loops of BTFCO thin films.

As shown in Fig. 6a, the electric hysteresis loops of BFO, BTFO and BTFCO thin films are measured at 1 kHz at room temperature. Saturated hysteresis loops with well-defined rectangularity of the Tb and Cr co-doped films are obtained. The remnant polarization of the co-doped films is much higher than that of pure BFO thin film ($2P_r$=2.08 μC/cm^2). The $2P_r$ of BTFO and BTFCO thin films are 124.52 (at 1052 kV/cm) and 161.60 μC/cm^2 (at 1010 kV/cm), respectively. In the pure BFO thin film, a substantial number of oxygen vacancies are created to compensate the positive charge deficiency caused by the vaporization of Bi and the reduction of the Fe^{3+} ions to Fe^{2+} [26]. Oxygen vacancy leads to structure distortion of the ABO_3 perovskite unit cell and the displacement of B-site ions inhibited, resulting in the reduction of the remnant polarization. As shown in Fig. 6b, the evolution of the *P–E* hysteresis loops measured at 1 kHz during the course of increasing the applied voltage from 10 V to 80 V. As the applied voltage increases, it can be found that both the P_r and E_c increase and then become saturated for the electric field higher than 1000 kV/cm.

Furthermore, the increase of $2P_r$ of the co-doped thin films is consistent with the measured lower leakage current densities

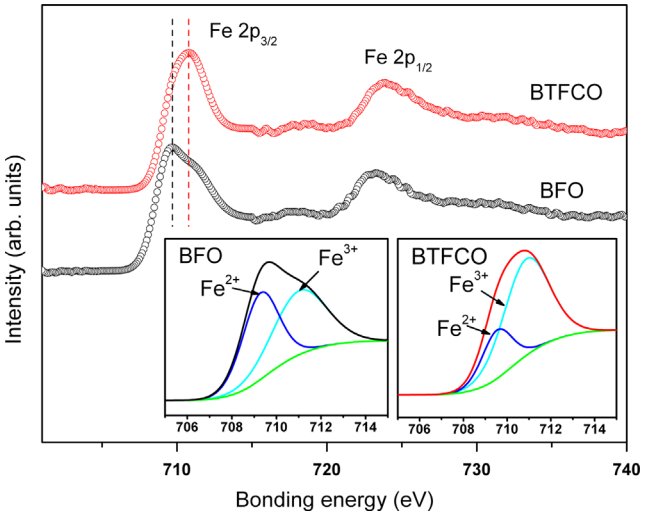

Fig. 7. XPS spectra of Fe ions in the BFO and BTFCO thin films. The insets show that the Fe $2p_{3/2}$ state contains most contributions from the Fe^{3+} ion states.

compared with that of pure BFO thin film. In our study, due to the higher crystallization and relatively good film quality, the structure transition and (110) preferred orientation are observed in XRD analysis and Raman spectroscopy. The structure transition might be one of the main reasons for the large ferroelectric polarization of the samples.

The oxidation states of Fe in BFO and BTFCO thin films are investigated by XPS, and the Fe 2p peaks of BFO and BTFCO thin films are shown in Fig. 7. The positions of Fe $2p_{3/2}$ lines are at around 710 eV, which means the coexistence of both Fe^{3+} and Fe^{2+} states. The Fe $2p_{3/2}$ line of BTFCO thin film shifts a little to higher bonding energy in comparison with the BFO, implying the higher content in Fe^{3+}. By fitting the peaks for the valence state of Fe ions, the ratios of Fe^{2+}/Fe^{3+} in the BFO and BTFCO thin films are calculated as 45:55 and 26:74 respectively, indicating that BTFCO film has less Fe^{2+} ions. This might also be evidence for the decrease of oxygen vacancies, corresponding to the lower leakage current density in BTFCO thin film [27]. In other words, Tb and Cr co-doping favors the decrease of oxygen vacancies in BFO thin film, resulting in ferroelectric property enhancement.

4. Conclusions

BFO, BTFO and BTFCO thin films are successfully prepared by a sol–gel method. XRD patterns and Raman spectroscopy reveal that BTFCO thin film shows the structure transition and (110) preferred orientation. The co-doped BTFCO thin film exhibits the improved electrical properties, the lower leakage current density (3.76×10^{-5} A/cm^2 at 200 kV/cm), the higher dielectric constant (160 at 1 MHz) and the lower dielectric loss (0.14 at 1 MkHz). The ratios of Fe^{2+}/Fe^{3+} in the BFO and BTFCO thin films are calculated as 45:55 and 26:74 respectively, indicating that the presence of Fe^{2+} ions is suppressed in the BTFCO film. Furthermore, a giant remnant polarization value ($2P_r = 161.60$ μC/cm^2) and the better saturated ferroelectric hysteresis loops are observed in BTFCO thin film. These results can be explained by structure transition and effective reduction of oxygen vacancies. All these enhanced properties make this combination ideal for practical applications.

Acknowledgments

This work was supported by the Project of the National Natural Science Foundation of China (Grant no. 51172135); the Young Scientists Fund of the National Natural Science Foundation of China (Grant no. 51002092); Research and Special Projects of the Education Department of Shaanxi Province (Grant no. 12JK0445); the Graduate Innovation Fund of Shaanxi University of Science & Technology (SUST-A04).

References

[1] W. Eerenstein, N.D. Mathur, J.F. Scott, Multiferroic and magnetoelectric materials, Nature 442 (2006) 759–765.
[2] M.K. Singh, H.M. Jang, S. Ryu, M.-H. Jo, Polarized, Raman scattering of multiferroic $BiFeO_3$ epitaxial films with rhombohedral R3c symmetry, Applied Physics Letters 88 (2006) 042907–042909.
[3] J. Wang, J.B. Neaton, H. Zheng, V. Nagarajan, S.B. Ogale, B. Liu, D. Viehland, V. Vaithyanathan, D.G. Schlom, U.V. Waghmare, N.A. Spaldin, K.M. Rabe, M. Wuttig, R. Ramesh, Epitaxial $BiFeO_3$ multiferroic thin film heterostructures, Science 299 (2003) 1719–1722.
[4] J.G. Wu, J. Wang, Improved ferroelectric behavior in (110) oriented $BiFeO_3$ thin films, Journal of Applied Physics 107 (2010) 034103.
[5] X.Z. Wang, H.R. Liu, B.W. Yan, Enhanced ferroelectric properties of Ce-substituted $BiFeO_3$ thin films prepared by sol–gel process, Journal of Sol–Gel Science and Technology 47 (2008) 124–127.
[6] X. Xue, G.Q. Tan, H.J. Ren, A. Xia, Structural, electric and multiferroic properties of Sm-doped $BiFeO_3$ thin films prepared by the sol–gel process, Ceramics International 39 (2013) 6223–6228.
[7] J.K. Kim, S.S. Kim, W.J. Kim, A.S. Bhalla, Substitution effects on the ferroelectric properties of $BiFeO_3$ thin films prepared by chemical solution deposition, Journal of Applied Physics 101 (2007) 014108.
[8] S.U. Lee, S.S. Kim, M.H. Park, J.W. Kim, H.K. Jo, W.-J. Kim, Effects of co-substitution on the electrical properties of $BiFeO_3$ thin films prepared by chemical solution deposition, Applied Surface Science 254 (2007) 1493–1497.
[9] C.R. Foschini, M.A. Ramirez, S.R. Simoes, J.A. Varela, E. Longo, A.Z. Simoes, Piezoresponse force microscopy characterization of rare-earth doped $BiFeO_3$ thin films grown by the soft chemical method, Ceramics International 39 (1) (2013) 2185–2195.
[10] B.F. Yu, M.Y. Li, J. Wang, L. Pei, D.Y. Guo, X.Z. Zhao, Enhanced electrical properties in multiferroic $BiFeO_3$ ceramics co-doped by La^{3+} and V^{5+}, Journal of Physics D: Applied Physics 41 (2008) 185401–185403.
[11] T. Kawae, H. Tsuda, H. Naganuma, S. Yamada, M. Kumeda, S. Okamura, A. Morimoto, Composition dependence in $BiFeO_3$ film capacitor with suppressed leakage current by Nd and Mn cosubstitution and their ferroelectric properties, Japanese Journal of Applied Physics 47 (2008) 7586–7589.
[12] T. Kawae, Y. Terauchi, H. Tsuda, M. Kumeda, A. Morimoto, Improved leakage and ferroelectric properties of Mn and Ti codoped $BiFeO_3$ thin films, Applied Physics Letters 94 (2009) 112904–112906.
[13] Z. Wen, X. Shen, D. Wu, Q.Y. Xu, J.L. Wang, A.D. Li, Enhanced ferromagnetism at the rhombohedral–tetragonal phase boundary in Pr and Mn co-substituted powders, Solid State Communications 150 (2010) 2081–2084.

[14] D. Hong, S.W. Yu, J.R. Cheng, Sm–Ti co-substituted $BiFeO_3$ thin films prepared by sol–gel technique, Current Applied Physics 11 (2011) 255–259.
[15] Z. Wen, L. You, X. Shen, X.F. Li, D. Wu, J.L. Wang, A.D. Li, Multiferroic properties of $(Bi_{1-x}Pr_x)(Fe_{0.95}Mn_{0.05})O_3$ thin films, Materials Science and Engineering B 176 (2011) 990–995.
[16] X. Qi, J. Dho, R. Tomov, M.G. Blamire, J.L. MacManus-Driscoll, Greatly reduced leakage current and conduction mechanism in aliovalent-ion-doped $BiFeO_3$, Applied Physics Letters 86 (2005) 062903.
[17] X.M. Chen, G.D. Hu, W.B. Wu, C.H. Yang, X. Wang, Large piezoelectric coefficient in Tb-doped $BiFeO_3$ films, Journal of American Ceramic Society 93 (2010) 948–950.
[18] J.G. Wu, J. Wang, D.Q. Xiao, J.G. Zhu, $BiFeO_3/Zn_{1-x}Mn_xO$ bilayered thin films, Applied Surface Science 258 (2011) 1390–1394.
[19] P. Hermet, M. Goffinet, J. Kreisel, P. Ghosez, Raman and infrared spectra of multiferroic bismuth ferrite from first-principles, Physical Review B 75 (2007) 220102(R).
[20] P. Kharel, S. Talebi, B. Ramachandran, A. Dixit, V.M. Naik, M.B. Sahana, C. Sudakar, R. Naik, M.S.R. Rao, G. Lawes, Structural, magnetic, and electrical studies on polycrystalline transition-metal-doped $BiFeO_3$ thin films, Journal of Physics: Condensed Matter 21 (2009) 036001.
[21] C.F. Chung, J.P. Lin, J.M. Wu, Influence of Mn and Nb dopants on electric properties of chemical-solution-deposited $BiFeO_3$ films, Applied Physics Letters 88 (2006) 242909–242911.
[22] G.L. Song, H.X. Zhang, T.X. Wang, H.G. Yang, F.G. Chang, Effect of Sm, Co codoping on the dielectric and magnetoelectric properties of $BiFeO_3$ polycrystalline ceramics, Journal of Magnetism and Magnetic Materials 324 (2012) 2121–2426.
[23] G.Z. Liu, G. Wang, C.C. Wang, J. Qiu, M. He, J. Xing, K.J. Jin, H.B. Lu, G.Z. Yang, Effects of interfacial polarization on the dielectric properties of $BiFeO_3$ thin film capacitors, Applied Physics Letters 92 (2008) 122903–122905.
[24] R. Thomas, J.F. Scott, D.N. Bose, R.S. Katiyar, Multiferroic thin-film integration onto semiconductor devices, Journal of Physics: Condensed Matter 22 (2010) 423201.
[25] Q. Ke, X. Lou, Y. Wang, J. Wang, Oxygen-vacancy-related relaxation and scaling behaviors of $Bi_{0.9}La_{0.1}Fe_{0.98}Mg_{0.02}O_3$ ferroelectric thin films, Physical Review B 82 (2010) 024102–024104.
[26] K. Abe, N. Sakai, J. Takahashi, H. Itoh, N. Adachi, T. Ota, Leakage current properties of cation-substituted $BiFeO_3$ ceramics, Japanese Journal of Applied Physics 49 (2010) 09MB01.
[27] W. Yao, C.W. Nan, Enhanced ferroelectricity in Ti-doped multiferroic $BiFeO_3$ thin films, Applied Physics Letters 89 (2006) 052903–052905.